

# Quantitative Methods in Phase-Contrast X-Ray Imaging

T.E. Gureyev, A.W. Stevenson, D. Paganin, S.C. Mayo, A. Pogany, D. Gao, and S.W. Wilkins

**A new method for extracting quantitative information from phase-contrast x-ray images obtained with microfocus x-ray sources is presented. The proposed technique allows rapid noninvasive characterization of the internal structure of thick optically opaque organic samples. The method does not generally involve any sample preparation and does not need any x-ray optical elements (such as monochromators, zone plates, or interferometers). As a consequence, samples can be imaged in vivo or in vitro, and the images are free from optical aberrations. While alternative techniques of x-ray phase-contrast imaging usually require expensive synchrotron radiation sources, our method can be implemented with conventional, albeit microfocus, x-ray tubes, which greatly enhances its practicality. In the present work, we develop the theoretical framework, perform numerical simulations, and present the first experimental results, demonstrating the viability of the proposed approach. We believe that this method should find wide-ranging applications in clinical radiology and medical research.**

*Copyright © 2000 by W.B. Saunders Company*

**S**INCE THE ORIGINAL DISCOVERY by W.C. Röntgen in 1895, x-ray imaging has played a prominent and ever-expanding role as an analytical method in science, industry, and medical practice. The property of x-rays that sets them apart from most alternative techniques, is their ability to image the internal structure of thick optically opaque samples in their native state. Another important property is their direct sensitivity to chemical composition of the sample. In some cases, the dependence of x-ray image contrast on density or chemical composition can be quantified, and examples of such quantitative imaging are given in the present report.

From the practical point of view, the relative ease with which x-rays with useful energies can be generated and detected is also of crucial importance. Recently, impressive advances in x-ray science and applications have been achieved with the use of synchrotron radiation sources. Synchrotrons can generate x-rays with some desirable properties, for example, monochromatic and spatially coherent beams with extremely high brightness and tunable energy, but the average cost of a third-generation synchrotron is usually of the order of hundreds of millions of dollars. In the present report, we demonstrate that at least some of the applications previously considered possible only with synchro-

tron radiation can in fact be realized in the laboratory using conventional, albeit microfocus, x-ray sources. This may constitute a cost-reduction factor of the order of thousands in the basic instrument resources required. Moreover, we show that the use of microfocus laboratory sources results in some additional advantages not routinely available with synchrotron beamlines, such as inherent magnification of the image.

During its first 100 years, x-ray radiography has primarily relied on differential absorption of x-rays as a mechanism of contrast formation. As x-rays are electromagnetic waves, they must in principle also exhibit wave effects, such as refraction and diffraction. It is well known that Röntgen himself tried to demonstrate such wave effects with x-rays, but without success. The reason for his failure was, of course, the extreme weakness of refraction of x-rays in most materials. For the same reason, phase contrast has not been widely used in x-ray imaging until recently. In the second half of the 20th century, several methods have been developed for visualizing hard x-ray phase contrast produced by noncrystalline samples. Initially, these methods involved near-perfect crystals as optical elements, as for example, in x-ray interferometry<sup>1,2</sup> and single crystal-analyzer techniques.<sup>3-5</sup> More recently, the in-line method, which generally does not require any x-ray optics, has been suggested and implemented.<sup>6-9</sup> The last method, which is close in principle to Gabor's in-line holography,<sup>10</sup> is used in the present report. In some cases, and particularly for soft tissue, x-ray phase-contrast imaging (PCI) can produce much stronger contrast than conventional absorption-based techniques. Combined with appropriate computer processing, PCI can also deliver some further benefits, such as rapid quantitative imaging in different modalities. It can also be easily merged

---

*From CSIRO Manufacturing Science and Technology, Clayton South, Victoria, Australia.*

*Supported by X-Ray Technologies Pty Ltd, Fuji Film Co, and Bertholds (Australia).*

*Address reprint requests to T.E. Gureyev, MD, CSIRO Manufacturing Science and Technology, PB 33, Clayton South MDC, VIC. 3169, Australia. E-mail: T.Gureyev@cmst.csiro.au.*

*Copyright © 2000 by W.B. Saunders Company*

*0897-1889/00/1302-1029\$10.00/0*

*doi.10.1053/jdim.2000.6844*

with conventional tomographic techniques leading to three-dimensional phase-contrast imaging.

It should be noted, however, that compared with contact radiography, direct PCI images may be more difficult to interpret in terms of the sample features. Therefore, to achieve optimum information from in-line PCI images, interpretation, as a function of the properties of the source, the detector, and the imaging layout, is essential. Such interpretation is a nontrivial step on the way from a collected PCI image through computer-assisted image processing to quantitative characterization of the sample.<sup>11,12</sup> In order to demonstrate the computer processing steps that must be taken to extract the maximum possible amount of reliable information from the image, a good understanding of the mechanism of x-ray image formation is required. The fundamentals of in-line PCI physics are briefly described in the next section.

#### IN-LINE PHASE-CONTRAST IMAGE FORMATION

The interaction of an x-ray beam with a noncrystalline sample can usually be described in terms of line integrals of the complex refractive index,  $n_\lambda(x, y, z) = 1 - \delta_\lambda - i\beta_\lambda$  ( $\lambda$  is the wavelength). The real part,  $\delta_\lambda$ , of the refractive index is responsible for refraction, while the imaginary part,  $\beta_\lambda$ , determines absorption. Consider a plane monochromatic x-ray wave with unit intensity propagating along the direction of the optic axis  $z$  (Fig 1). Phase shifts,  $\varphi_\lambda(x, y, 0)$ , that the sample introduced into the transmitted x-ray beam are proportional to the projected values of the real part of the refractive index, while the distribution of the transmitted x-ray intensity immediately after the sample,  $I_\lambda(x, y, 0)$ , is proportional to projections of the imaginary part:

$$\varphi_\lambda(x, y, 0) = -(2\pi/\lambda) \int_{-\infty}^0 \delta_\lambda(x, y, z') dz', \quad (1)$$

$$I_\lambda(x, y, 0) = \exp \left\{ -(4\pi/\lambda) \int_{-\infty}^0 \beta_\lambda(x, y, z') dz' \right\}. \quad (2)$$

As conventional radiographs represent the absorption maps,  $I_\lambda(x, y, 0)$ , they can only provide information about the imaginary part of the refractive index, and they are insensitive to its real part. Another important point to be noted is the different dependence of  $\beta_\lambda$  and  $\delta_\lambda$  on wavelength (energy) of x-rays:  $\beta_\lambda \sim \lambda^4$  and  $\delta_\lambda \sim \lambda^2$  away from absorption

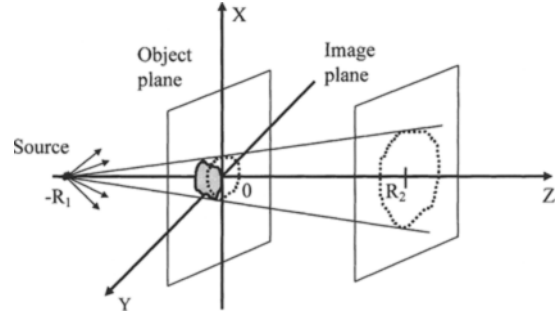


Fig 1. Generic scheme of in-line imaging.

edges.<sup>13</sup> Therefore, phase (refraction) effects dominate absorption effects at shorter wavelengths (higher x-ray energies).

It is well known in medical radiography that an increase of the distance between the sample under examination and the x-ray detector (film) usually leads to blurring of x-ray images due to the finite size of the x-ray source. In the in-line method of PCI, the size of the x-ray source is significantly reduced (typically to  $<40 \mu\text{m}$ ). This allows refraction effects to be visualised and provides information about the distribution of the real part of complex refractive index in the sample. To optimize phase contrast, a significant distance (of the order of 0.1 to 1 m) between the sample and the detector is typically required in PCI using hard x-rays with wavelength of the order of  $1 \text{ \AA}$  or shorter (energy  $\sim 10 \text{ keV}$  or higher).

The formation of phase contrast in PCI can normally be described by the transport of intensity equation (TIE):<sup>14-17</sup>

$$-\nabla \cdot [I_\lambda(x, y, 0)\nabla\varphi_\lambda(x, y, 0)] = 2\pi/(R\lambda)[I_\lambda(x, y, R) - I_\lambda(x, y, 0)], \quad (3)$$

where  $\nabla = (\partial_x, \partial_y)$  is the gradient operator and  $R$  is the object-to-detector distance (in the case of a point source,  $R$  is replaced by  $R_1R_2/(R_1 + R_2)$ , where  $R_1$  is the source-to-object distance and  $R_2$  is the object-to-detector distance, see Fig 1 and Wilkins et al<sup>8</sup>).

Equation 3 implies that the contrast of images collected at some distance from the object is proportional to that distance and to the magnitude of phase shifts introduced by the sample into the transmitted x-ray beam. As the contrast is actually proportional to derivatives of the phase distribution in the object plane, in practice, PCI images often display naturally "edge-enhanced" contrast. While

the presence of characteristic sharp black-white fringes at the regions corresponding to rapid change of refractive index can be useful for detection of particular features in the sample, in general it means that the relationship between the refractive index and the image contrast in PCI is more complicated than in conventional radiography. This calls for the application of appropriate 'reconstruction' techniques.

From Equation 3 it follows that in the case of a nonabsorbing sample ( $I_\lambda(x, y, 0) \equiv I_\lambda(0)$ ), the projected distribution,  $\varphi_\lambda(x, y, 0)$ , of  $\delta_\lambda$  can be obtained by "inverse-Laplace" filtering of a single PCI image intensity,  $I_\lambda(x, y, R)$ .<sup>16</sup> In the general case, the projected values of both the real and imaginary parts of the refractive index can be obtained from Equation 3, where there are two unknown distributions,  $I_\lambda(x, y, 0)$  and  $\varphi_\lambda(x, y, 0)$ . Consequently, at least two different images are required for the unambiguous reconstruction of the projected complex refractive index. Such images can be collected at two different distances,  $R$  and  $R + \delta R$ , from the sample.<sup>16-18</sup> As it follows from Equation 1, the reconstructed phase images may be identified with quantitative maps of projected distribution of the real part of the complex refractive index. In medical radiography, these maps can be used directly to determine the projected spatial distribution of density in the samples.

It has been demonstrated that a high spatial coherence of x-rays is the only critical prerequisite for PCI, while the tolerance to spectral incoherence (polychromaticity) is much higher.<sup>8</sup> At synchrotrons, a high degree of coherence (collimation and monochromaticity) of x-rays is achieved by means of highly sophisticated methods of x-ray production. As far as the spatial coherence is concerned, one can view a laboratory microfocus x-ray source as a cheap and efficient alternative to synchrotron radiation.

#### PCI IMAGES AND THEIR PROCESSING

First, we demonstrate how the image processing in accordance with the presented theory can be used to analyze PCI images. Figure 2A is an image of a polystyrene sphere of approximately 118  $\mu\text{m}$  in diameter obtained at the European Synchrotron Radiation Facility (ESRF) using x-rays with energy  $E = 19.6$  keV ( $\lambda \approx 0.63$   $\text{\AA}$ ).<sup>19</sup> The image was collected at  $R = 15$  cm object-to-detector distance. A corresponding contact radiograph showed no

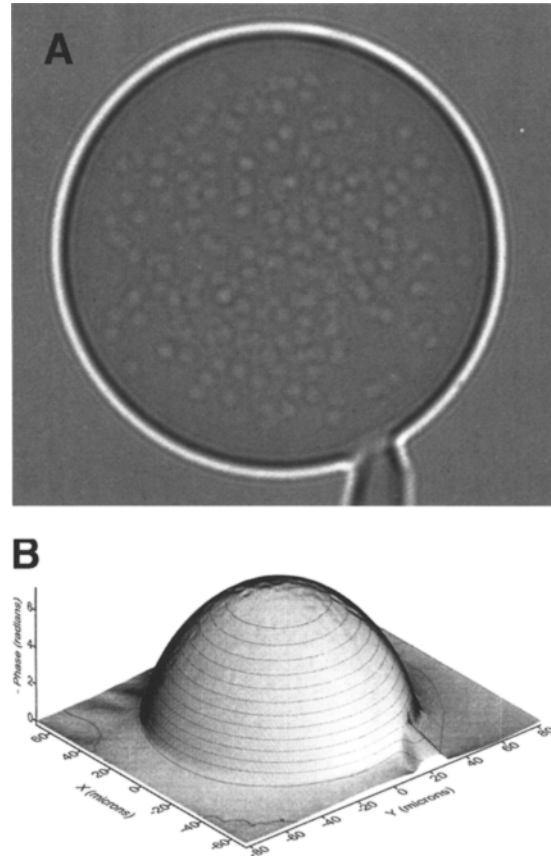


**Fig 2.** (A) Experimental in-line image of a polystyrene sphere (image obtained by C. Raven at ESRF ID 22). (B) Phase-reconstructed image of the polystyrene sphere shown in (A).

absorption contrast, as 118  $\mu\text{m}$  of polystyrene has negligible (0.25%) absorption at the chosen X-ray energy. Therefore, all of the contrast visible in Fig 2A is phase contrast. The strong black-white fringes near the edges of the sphere and the supporting pin correspond to the phase Laplacian as predicted by Equation 3. Some defects (air bubbles) are clearly visible in the interior of the sphere. On the other hand, the overall shape (thickness variation) cannot be directly determined from Fig 2A. Figure 2B shows an inverse-Laplace filtered version of Fig 2A. According to Equation 3, Fig 2B displays the variations of the phase,  $\varphi_\lambda(x, y, 0)$ , in the object plane, or, equivalently, the projected values of the real part of the refractive index distribution in the sphere. The values of the phase shifts obtained from Fig 2B are in a very good agreement with the theoretical estimation obtained using Equation 1 for an ideal polystyrene ( $\delta = 6.1 \times 10^{-7}$ ) sphere

with 118  $\mu\text{m}$  diameter and radiation  $E = 19.6$  keV.<sup>19</sup> Therefore, processing of an in-line x-ray image in accordance with the theory of PCI contrast formation allows one to obtain some important qualitative information (eg, the true shape), as well as quantitative data about the internal composition of the sample.

The remaining images were obtained using a laboratory microfocus x-ray source (Feinfocus Röntgen-Systeme GmbH, Garbsen, Germany, Model FXE-225.20 with W target, operating at  $V = 30$  kV) and Fuji Imaging Plates scanned using BAS-5000 as detection media. The very large linear dynamic range of Imaging Plates makes them suitable for quantitative in-line PCI. Figure 3A

shows human finger bones with many fine details of trabecular structure visible. Spatial resolution of Fig 3A was approximately 6  $\mu\text{m}$ . Figure 3B shows a magnified subregion ( $1,024 \times 1,024$  pixels) of Fig 3A. The image contrast in Figs 3A and B represents a combination of absorption and phase contrasts. In Fig 3C, we demonstrate the result of numerical processing of the image from Fig 3B in accordance with Equation 3. This processed image represents the true map of the projected mass distribution in the sample. The approximate range of the reconstructed values is between 0.23 mm and 0.27 mm of solid apatite ( $\text{Ca}_5(\text{PO}_4)_3\text{OH}$ ).

Finally, Fig 4 demonstrates the capability of the PCI technique for imaging of soft tissues. Pre-

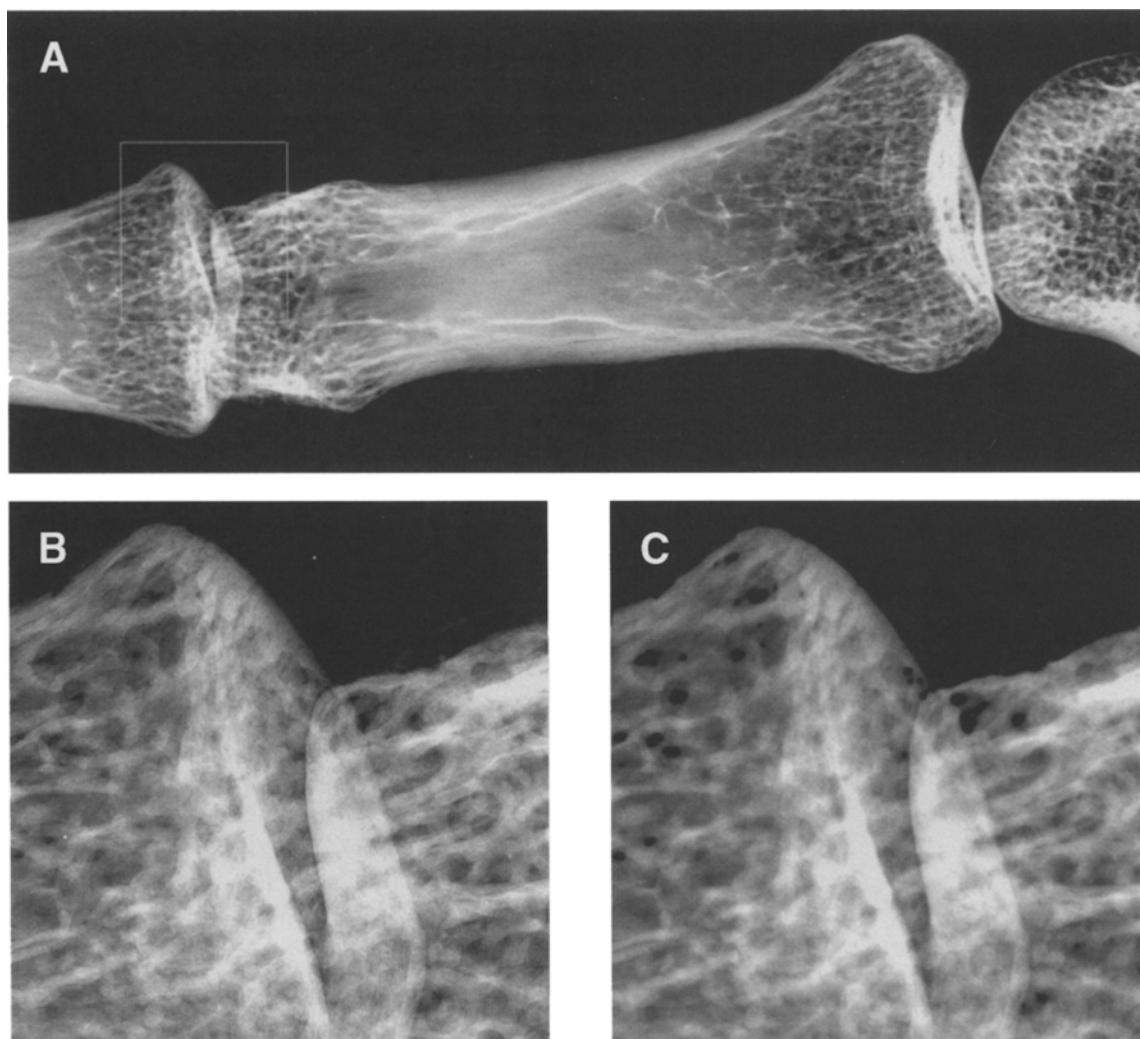


**Fig 3.** (A) Experimental in-line image of dry human finger bones. (B) Magnified subregion of (A). (C) Reconstructed map of projected mass distribution in region (B).

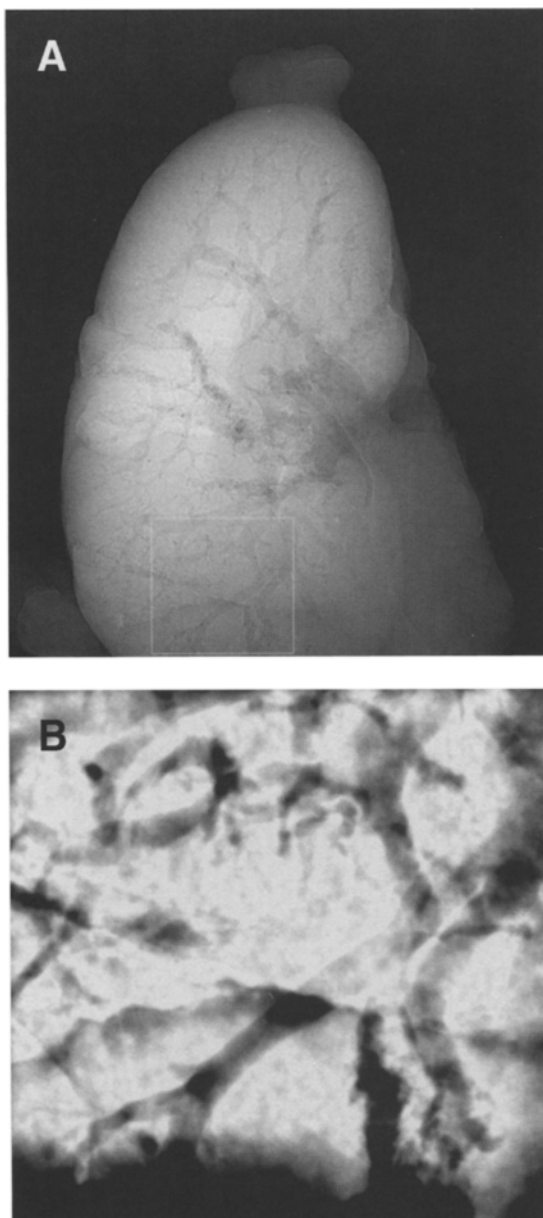


**Fig 4. (A) Experimental in-line image of a wet mouse kidney. (B) Reconstructed map of projected mass distribution in a subregion of (A).**

sented in Fig 4A is a kidney of a mouse, again showing a combination of absorption and phase contrast. The spatial resolution here is approximately  $4 \mu\text{m}$ . Figure 4B contains a processed version of a  $1,024 \times 1,024$  pixel region of Fig 4A outlined by a white square. The processing consisted of inversion of Equation 3 followed by the background subtraction to remove the intensity gradient due to the x-ray source. The approximate range of the reconstructed projected mass distribution as shown in Fig 4B is between 2.6 mm and 2.8 mm of water.

The results presented in Figs 3 and 4 are preliminary. We are currently working on procedures that will ensure accurate and rapid quantitative information extraction from in-line hard x-ray images obtained with a laboratory polychromatic microfocus source.

## CONCLUSIONS

We have demonstrated some key features of a new technique, in-line phase-contrast imaging with hard x-rays, for imaging of organic samples using a laboratory microfocus source and no x-ray optics. This technique can produce high-contrast images of objects and features composed of light chemical elements, eg, biological samples. The method can be applied to thick optically opaque samples in their native state. Using a microfocus laboratory x-ray source, it is easy to obtain a large field of view and variable geometrical magnification, while preserving a very large depth of field (of the order of meters). We explained how numerical processing of the experimental PCI images in accordance with the mathematical equations describing the image formation can be utilized to obtain reliable and meaningful quantitative information about the internal structure of the samples. In particular, we showed that the “phase-reconstructed” PCI images have a direct quantitative relationship to the spatial density distribution in the sample. We believe that this method should find wide ranging applications in clinical radiology and medical research.

## REFERENCES

1. Bonse U, Hart M: An x-ray interferometer. *Appl Phys Lett* 6:155-156, 1965
2. Momose A, Takeda T, Itai Y: Phase-contrast x-ray computed tomography for observing biological specimens and organic materials. *Rev Sci Instrum* 66:1434-1436, 1995
3. Forster E, Goetz K, Zaumseil P: Double crystal diffractometry for the characterization of targets for laser fusion experiments. *Kristall und Technik* 15:937-945, 1980
4. Ingal VN, Beliaevskaya EA: X-ray plane-wave topography observation of the phase contrast from a non-crystalline object. *J Phys D Appl Phys* 28:2314-2317, 1995
5. Davis T, Gao D, Gureyev T, et al: Phase-contrast imaging

of weakly absorbing materials using hard x-rays. *Nature* 373:595-598, 1995

6. Wilkins SW: Simplified conditions and configurations for phase-contrast imaging with hard x-rays. Australian Patent Application, filed March 28, 1995 (PN 2112/95); PCT Application, filed March 28, 1996

7. Snigirev A, Snigireva I, Kohn V, et al: On the possibilities of x-ray phase contrast microimaging by coherent high-energy synchrotron radiation. *Rev Sci Instrum* 66:5486-5492, 1995

8. Wilkins SW, Gureyev TE, Gao D, et al: Phase-contrast imaging using polychromatic hard x-rays. *Nature* 384:335-338, 1996

9. Cloetens P, Barrett R, Baruchel J, et al: Phase objects in synchrotron radiation hard x-ray imaging. *J Phys D Appl Phys* 29:133-146, 1996

10. Gabor D: A new microscopic principle. *Nature* 161:777-778, 1948

11. Pogany A, Gao D, Wilkins SW: Contrast and resolution in imaging with a microfocus x-ray source. *Rev Sci Instrum* 68:2774-2782, 1997

12. Gao D, Pogany A, Stevenson AW, et al: Phase-contrast radiography. *Radiographics* 18:1257-1267, 1998

13. Arndt UW, Willis BTM: *Single Crystal Diffractometry*. Cambridge, UK, Cambridge University Press, 1966, p 185

14. Cowley JM: *Diffraction Physics*. Amsterdam, The Netherlands, North-Holland, 1995, pp 60-62

15. Teague MR: Deterministic Phase Retrieval: A Green's Function Solution. *J Opt Soc Am* 73:1434-1441, 1983

16. Gureyev TE, Wilkins SW: On x-ray phase imaging with a point source. *J Opt Soc Am A* 15:579-585, 1998

17. Gureyev TE: Transport of intensity equation for beams in arbitrary state of temporal and spatial coherence. *Optik* 110:263-266, 1999

18. Wilkins SW, Pogany A, Stevenson AW, et al: Phase retrieval in phase contrast imaging. PCT Patent Application PCT/AU97/00882, filed Dec 24, 1997 with priority date December 24, 1996

19. Gureyev TE, Raven C, Snigirev A, et al: Hard x-ray quantitative non-interferometric phase-contrast microscopy. *J Phys D Appl Phys* 32:563-567, 1999